

Study of anomalous quartic $WW\gamma\gamma$ couplings at the Compact Linear Collider

M. Köksal*

Department of Physics, Cumhuriyet University, 58140, Sivas, Turkey

Abstract

We have examined the sensitivities to the anomalous quartic $WW\gamma\gamma$ gauge boson coupling by investigating the three different processes $e^+e^- \rightarrow W^-W^+\gamma$, $e^+e^- \rightarrow e^+\gamma^*e^- \rightarrow e^+W^-\gamma\nu_e$, and $e^+e^- \rightarrow e^+\gamma^*\gamma^*e^- \rightarrow e^+W^-W^+e^-$ at the CLIC. We obtained 95% confidence level bounds on the anomalous coupling parameters $\frac{a_0}{\Lambda^2}$ and $\frac{a_c}{\Lambda^2}$ with various values of the integrated luminosity and center-of-mass energy. We have shown that the best bounds obtained on the anomalous coupling parameters $\frac{a_c}{\Lambda^2}$ and $\frac{a_0}{\Lambda^2}$ from these reactions are at the order of 10^{-7} and 10^{-8} GeV^{-2} , respectively, which are about two orders of magnitude better than the CMS bounds.

arXiv:1402.3112v1 [hep-ph] 13 Feb 2014

*mkoksal@cumhuriyet.edu.tr

I. INTRODUCTION

In the Standard Model (SM) of particle physics, triple and quartic interactions of the gauge bosons have not been determined with great accuracy. The possible deviation of gauge boson self-interactions from the SM predictions will be an important sign of new physics beyond the SM. A simple way of new physics research is the effective Lagrangian method. This fundamental theory, which is independent of the details of the model, reduces to the SM at lower energies. The genuine quartic gauge couplings occur with effective operators which do not induce new trilinear vertices. Hence, quartic gauge couplings are interchanged by genuine quartic gauge couplings while trilinear gauge boson couplings are equal to SM values. Therefore, we consider that genuine quartic gauge couplings can be separately examined from the effects occurring in trilinear gauge couplings. C and P conserving dimension 6 effective Lagrangian for genuine quartic $WW\gamma\gamma$ couplings are given by [1–3]

$$L = L_0 + L_c, \quad (1)$$

$$L_0 = \frac{-\pi\alpha}{4} \frac{a_0}{\Lambda^2} F_{\mu\nu} F^{\mu\nu} W_\alpha^{(i)} W^{(i)\alpha}, \quad (2)$$

$$L_c = \frac{-\pi\alpha}{4} \frac{a_c}{\Lambda^2} F_{\mu\alpha} F^{\mu\beta} W^{(i)\alpha} W_\beta^{(i)} \quad (3)$$

where $W^{(i)}$ is $SU(2)_W$ triplet, $F_{\mu\nu} = \partial_\mu A_\nu - \partial_\nu A_\mu$ is the tensor for electromagnetic field strength, Λ is the scale of the new physics, and a_0 and a_c are the dimensionless anomalous coupling constants.

In the presence of the effective Lagrangian in Eqs.(2-3), the vertex functions for $W^+(k_1^\mu)W^-(k_2^\nu)\gamma(p_1^\alpha)\gamma(p_2^\beta)$ are obtained respectively by

$$i \frac{2\pi\alpha}{\Lambda^2} a_0 g_{\mu\nu} [g_{\alpha\beta}(p_1 \cdot p_2) - p_{2\alpha} p_{1\beta}], \quad (4)$$

$$i \frac{\pi\alpha}{2\Lambda^2} a_c [(p_1 \cdot p_2)(g_{\mu\alpha} g_{\nu\beta} + g_{\mu\beta} g_{\alpha\nu}) + g_{\alpha\beta}(p_{1\mu} p_{2\nu} + p_{2\mu} p_{1\nu}) - p_{1\beta}(g_{\alpha\mu} p_{2\nu} + g_{\alpha\nu} p_{2\mu}) - p_{2\alpha}(g_{\beta\mu} p_{1\nu} + g_{\beta\nu} p_{1\mu})]. \quad (5)$$

Measurements made by the OPAL, D0 and CMS collaborations provide experimental bounds on anomalous quartic $WW\gamma\gamma$ couplings. The bounds at 95% C. L. on anomalous $\frac{a_0}{\Lambda^2}$ and $\frac{a_c}{\Lambda^2}$ couplings through the processes $e^+e^- \rightarrow W^-W^+\gamma$ and $e^+e^- \rightarrow \nu\bar{\nu}\gamma\gamma$ by the OPAL collaboration at LEP2 collider are given by $-0.020 \text{ GeV}^{-2} < \frac{a_0}{\Lambda^2} < 0.020 \text{ GeV}^{-2}$, $-0.052 \text{ GeV}^{-2} < \frac{a_c}{\Lambda^2} < 0.037 \text{ GeV}^{-2}$ [4]. Also, the current bounds on anomalous $\frac{a_0}{\Lambda^2}$ and $\frac{a_c}{\Lambda^2}$ couplings have been provided using WWA with the help of the process $pp(\bar{p}) \rightarrow p\gamma^*\gamma^*p(\bar{p}) \rightarrow pW^-W^+p(\bar{p})$ by D0 collaboration at the Tevatron [5] and CMS collaboration at the LHC [6]. The anomalous couplings were obtained by D0 collaboration

$$-0.00043 \text{ GeV}^{-2} < \frac{a_0}{\Lambda^2} < 0.00043 \text{ GeV}^{-2}, \quad (6)$$

$$-0.0016 \text{ GeV}^{-2} < \frac{a_c}{\Lambda^2} < 0.0015 \text{ GeV}^{-2}. \quad (7)$$

The most restrictive bounds on the parameters of quartic anomalous $WW\gamma\gamma$ couplings were determined by CMS collaboration

$$-4.0 \times 10^{-6} \text{ GeV}^{-2} < \frac{a_0}{\Lambda^2} < 4.0 \times 10^{-6} \text{ GeV}^{-2}, \quad (8)$$

$$-1.5 \times 10^{-5} \text{ GeV}^{-2} < \frac{a_c}{\Lambda^2} < 1.5 \times 10^{-5} \text{ GeV}^{-2}. \quad (9)$$

In the literature, anomalous quartic $WW\gamma\gamma$ couplings at the linear colliders were studied through the processes $e^+e^- \rightarrow VVV$ [7–10], $e^+e^- \rightarrow VVFF$ [11], $e\gamma \rightarrow VVF$ [12, 13], and $\gamma\gamma \rightarrow VVV$ [14, 15] where $V = Z, W^\pm$ or γ and $F = e$ or ν . In addition, these couplings were examined at the LHC via the processes $pp \rightarrow p\gamma^*\gamma^*p \rightarrow pW^-W^+p$ [16, 17], $pp \rightarrow p\gamma^*p \rightarrow pW\gamma qX$ [18], $pp \rightarrow W\gamma\gamma$ [19–21] and $qq \rightarrow qq\gamma\gamma$ [22].

In this study, we probe the anomalous quartic $WW\gamma\gamma$ gauge boson coupling by analyzing the three different processes $e^+e^- \rightarrow W^-W^+\gamma$, $e^+e^- \rightarrow e^+\gamma^*e^- \rightarrow e^+W^-\gamma\nu_e$, and $e^+e^- \rightarrow e^+\gamma^*\gamma^*e^- \rightarrow e^+W^-W^+e^-$ at the CLIC.

The Large Hadron Collider (LHC) may not be an appropriate platform to investigate genuine quartic gauge couplings due to remnants of usual pp deep inelastic processes. On the other hand, since e^- and e^+ are fundamental particles, linear e^-e^+ colliders can determine anomalous quartic gauge couplings parameters with much higher precision measurements than hadron colliders. The Compact Linear Collider (CLIC), which has high energy and luminosity, is a foreseen linear collider. It is expected to be built by realizing collisions in

three main stages of 0.5, 1.5, and 3 TeV [23]. The fundamental parameters of the three energy options are given in Table I. In the CLIC's first research region, high precision with different observables of the SM Higgs boson, top quark and gauge bosons, the characteristics provide opportunities to be determined. The second phase will enable the discovery of new physics beyond the SM. In addition, Higgs boson properties such as the Higgs self-coupling and rare Higgs decay modes will be examined. The third phase, which has a maximum energy of 3 TeV, is considered to be able to make the most accurate measurements of the SM, and to directly determine the pair-production of new heavy particles of mass up to 1.5 TeV [24].

The linear e^-e^+ collider also has $e\gamma$ and $\gamma\gamma$ options to examine the new physics research. $e\gamma$ and $\gamma\gamma$ being where high energy real photons can be obtained by converting the incoming leptons beam into a photon beam via the Compton backscattering mechanism [25–27]. In addition, the linear collider allows us to study photon-induced $e\gamma^*$ and $\gamma^*\gamma^*$ reactions arising from almost real photons. Here, γ^* is emitted by any of the incoming leptons and immediately after it collides with the other lepton. Hence, to some extent it is possible to investigate $e\gamma^*$ and $\gamma^*\gamma^*$ collisions at the CLIC. The photons in these processes have been described as a suitable framework by the Weizsacker-Williams approximation (WWA) [28–33]. The virtuality of these photons is very low and they are assumed to be almost real. Therefore, the photons are scattered at small angles along the e^- or e^+ beam paths. As a result, $e\gamma^*$ and $\gamma^*\gamma^*$ processes are produced in a natural way from the e^-e^+ process itself. Representative diagrams defining these processes are given in Figs. 1 and 2. In the literature, photon-induced reactions through the WWA have been widely examined at the LEP, Tevatron, and LHC [34–60].

II. CROSS SECTIONS

The processes $e^+e^- \rightarrow W^-W^+\gamma$, $e^+e^- \rightarrow e^+\gamma^*e^- \rightarrow e^+W^-\gamma\nu_e$, and $e^+e^- \rightarrow e^+\gamma^*\gamma^*e^- \rightarrow e^+W^-W^+e^-$ at the CLIC are described by tree-level Feynman diagrams as shown in Figs. 3-5. We can see from these figures that while the only one of these diagrams involves anomalous $WW\gamma\gamma$ vertex, the others show the contributions arising from the SM. We have used the COMPHEP-4.5.1 program for numerical calculations in this study [61]. In addition, we assume that while only one of the anomalous couplings is equal to zero at any given

time throughout our study, the other is non-zero. The total cross sections as functions of anomalous $\frac{a_0}{\Lambda^2}$ and $\frac{a_c}{\Lambda^2}$ couplings for these processes at the CLIC with $\sqrt{s} = 0.5, 1.5$ and 3 TeV are given in Figs. 6-14. We observe from Figs. 6-14 that the value of the anomalous cross section containing $\frac{a_0}{\Lambda^2}$ is larger than the value of the $\frac{a_c}{\Lambda^2}$ coupling. Hence, the obtained bounds on the $\frac{a_0}{\Lambda^2}$ coupling are anticipated to be more restricted than the bounds on $\frac{a_c}{\Lambda^2}$ coupling.

III. LIMITS ON THE ANOMALOUS COUPLINGS

During statistical analysis, we determined 95% confidence level bounds on the anomalous coupling parameters $\frac{a_0}{\Lambda^2}$ and $\frac{a_c}{\Lambda^2}$ a simple one-parameter χ^2 analysis when the number of SM events of the analyzed processes is greater than 10. The χ^2 analysis is defined by the following formula

$$\chi^2 = \left(\frac{\sigma_{SM} - \sigma_{NP}}{\sigma_{SM} \delta_{stat}} \right)^2 \quad (10)$$

where σ_{NP} is the total cross section in the existence of anomalous gauge couplings, $\delta_{stat} = \frac{1}{\sqrt{N}}$ is the statistical error: N is the number of events. First, the events number for the process $e^+e^- \rightarrow W^-W^+\gamma$ is given by

$$N = L_{int} \times \sigma_{SM} \times BR(W \rightarrow q\bar{q}') \times BR(W \rightarrow \ell\nu_\ell) \quad (11)$$

where L_{int} is the integrated luminosity and σ_{SM} is the SM cross section. The W boson is heavy enough to decay both hadronically and leptonically. It decays roughly 21.5% of the time leptonically (for electron or muon) and 67.6% of the time to hadrons. So we consider one of the W bosons decays leptonically and the other hadronically for the signal. Therefore, we consider that the branching ratio of the W bosons pairs in the final state to be $BR = 0.145$. In addition, we impose the acceptance cuts on the pseudorapidity $|\eta^\gamma| < 2.5$ and the transverse momentum $p_T^\gamma > 20$ GeV for the final state photon.

In Table II, we calculate bounds on the anomalous coupling parameters $\frac{a_0}{\Lambda^2}$ and $\frac{a_c}{\Lambda^2}$ for some luminosities and center-of-mass energies of the process $e^+e^- \rightarrow W^-W^+\gamma$. We observe from Table II that the obtained bounds on the anomalous couplings via the process $e^+e^- \rightarrow$

$W^-W^+\gamma$ with $\sqrt{s} = 0.5$ TeV are worse than best bounds attained by CMS collaboration. On the other hand, our bounds at 1.5 and 3 TeV of center-of-mass energies of the same process are, even at small luminosity values, better than the experimental bounds. Especially, we have found the bounds of the anomalous $\frac{a_0}{\Lambda^2}$ coupling as $[-9.96 \times 10^{-8}, 7.27 \times 10^{-8}]$ GeV $^{-2}$ while the bounds on $\frac{a_c}{\Lambda^2}$ coupling as $[-1.76 \times 10^{-7}, 1.31 \times 10^{-7}]$ GeV $^{-2}$ at the integrated luminosity of 590 fb $^{-1}$ and center-of-mass energy of 3 TeV.

In the second analysis, the events number for the process $e^+e^- \rightarrow e^+\gamma^*e^- \rightarrow e^+W^-\gamma\nu_e$ is obtained by

$$N = L_{int} \times \sigma_{SM} \times BR(W \rightarrow q\bar{q}'). \quad (12)$$

Here, the W boson can decay leptonically, but in this case there occurs a great uncertainty due to the production of two neutrinos in the final state of our process. For this reason, we consider the hadronic decay of the W boson. Also, we apply the cuts $p_T^\gamma > 20$ GeV and $|\eta^\gamma| < 2.5$ for the photon in the final state. We show sensitivity bounds on the anomalous $\frac{a_0}{\Lambda^2}$ and $\frac{a_c}{\Lambda^2}$ couplings for the process $e^+e^- \rightarrow e^+\gamma^*e^- \rightarrow e^+W^-\gamma\nu_e$ at various integrated luminosities and center-of-mass energies in Table III. As we can see from this table, the obtained best bounds on anomalous $\frac{a_0}{\Lambda^2}$ and $\frac{a_c}{\Lambda^2}$ couplings through the reactions $e^+e^- \rightarrow e^+\gamma^*e^- \rightarrow e^+W^-\gamma\nu_e$ are found to be $[-4.05 \times 10^{-7}, 4.02 \times 10^{-7}]$ GeV $^{-2}$ and $[-4.81 \times 10^{-7}, 6.82 \times 10^{-7}]$ GeV $^{-2}$, respectively for $L_{int} = 590$ fb $^{-1}$ and $\sqrt{s} = 3$ TeV at the CLIC. We have shown that the bounds on anomalous couplings improve approximately up to 10 times for $\frac{a_0}{\Lambda^2}$ and up to 40 times for $\frac{a_c}{\Lambda^2}$.

Finally, for the process $e^+e^- \rightarrow e^+\gamma^*\gamma^*e^- \rightarrow e^+W^-W^+e^-$, in order to get realistic results the number of events is found by

$$N = L_{int} \times \sigma_{SM} \times BR(W \rightarrow q\bar{q}') \times BR(W \rightarrow \ell\nu_\ell). \quad (13)$$

In Table IV, we give the sensitivity bounds of the $\frac{a_0}{\Lambda^2}$ and $\frac{a_c}{\Lambda^2}$ couplings for $e^+e^- \rightarrow e^+\gamma^*\gamma^*e^- \rightarrow e^+W^-W^+e^-$ at CLIC with $\sqrt{s} = 0.5, 1.5$ and 3 TeV. As shown this table, we realize that the sensitivities of anomalous $\frac{a_0}{\Lambda^2}$ and $\frac{a_c}{\Lambda^2}$ couplings are rapidly enhanced when the center-of-mass energy of the CLIC increases.

IV. CONCLUSIONS

The CLIC is a high energy and luminosity linear collider in the planning stage. Having the high energy of the CLIC is quite important in terms of new physics research beyond the SM. For example, quartic $WW\gamma\gamma$ gauge couplings are defined by dimension 6 effective Lagrangian (2) and (3), and their energy dependences are very high. Hence, the processes including the $WW\gamma\gamma$ interactions have a higher momentum dependence with respect to the SM process. We can easily understand that the contribution to the cross section of anomalous quartic couplings quickly increases with the increase of center-of-mass energy. The analyzed processes that have very high energy and clean experimental environment, are anticipated to obtain a higher sensitivity of anomalous quartic gauge couplings. Therefore, we have studied the anomalous quartic gauge couplings in order to determine the bounds on the anomalous coupling parameters $\frac{a_0}{\Lambda^2}$ and $\frac{a_c}{\Lambda^2}$ by the processes $e^+e^- \rightarrow W^-W^+\gamma$, $e^+e^- \rightarrow e^+\gamma^*e^- \rightarrow e^+W^-\gamma\nu_e$, and $e^+e^- \rightarrow e^+\gamma^*\gamma^*e^- \rightarrow e^+W^-W^+e^-$ at the CLIC. We find out that the processes $e^+e^- \rightarrow W^-W^+\gamma$, $e^+e^- \rightarrow e^+\gamma^*e^- \rightarrow e^+W^-\gamma\nu_e$, and $e^+e^- \rightarrow e^+\gamma^*\gamma^*e^- \rightarrow e^+W^-W^+e^-$ at the CLIC with a center-of-mass energy of 3 TeV and a designed luminosity of 10 fb^{-1} can be investigated as anomalous $\frac{a_0}{\Lambda^2}$ and $\frac{a_c}{\Lambda^2}$ couplings with a better sensitivity than CMS. However, because up to now the best limits on anomalous $WW\gamma\gamma$ couplings are obtained with the aid of the process $pp \rightarrow p\gamma^*\gamma^*p \rightarrow pW^-W^+p$ using WWA at the LHC, probing anomalous couplings via $e^+e^- \rightarrow e^+\gamma^*e^- \rightarrow e^+W^-\gamma\nu_e$, and $e^+e^- \rightarrow e^+\gamma^*\gamma^*e^- \rightarrow e^+W^-W^+e^-$ at the CLIC would be quite interesting.

-
- [1] O. J. P. Eboli, M. C. Gonzalez-Garcia and S. F. Novaes, Nucl. Phys. B 411 381 (1994).
- [2] G. Belanger and F. Boudjema Phys. Lett. B 288, 201 (1992).
- [3] G. Belanger and F. Boudjema Phys. Lett. B 288, 210 (1992).
- [4] G. Abbiendi *et al.*, OPAL Collaboration, Phys. Rev. D 70 032005 (2004).
- [5] V. M. Abazov *et al.*, D0 Collaboration, Phys. Rev. D 88 012005 (2013).
- [6] S. Chatrchyan *et al.* CMS Collaboration, JHEP 1307 116 (2013).
- [7] G. Belanger, F. Boudjema, Y. Kurihara, D. Perret-Gallix, and A. Semenov, Eur. Phys. J. C 13 283-293 (2000).
- [8] W. J. Stirling and A. Werthenbach, Eur. Phys. J. C 14 103-110 (2000).
- [9] G. A. Leil and W. J. Stirling, J. Phys. G 21 517-524 (1995).
- [10] P.J. Dervan, A. Signer, W.J. Stirling, and A. Werthenbach, J. Phys. G 26 607-615 (2000).
- [11] W.J. Stirling and A. Werthenbach, Phys. Lett. B 466 369-374 (1999).
- [12] S. Atag and İ. Sahin, Phys. Rev. D 75 073003 (2007).
- [13] O. J. P. Eboli, M. C. Gonzalez-Garcia, and S. F. Novaes, Nucl. Phys. B 411 381-396 (1994).
- [14] O. J. P. Eboli, M. B. Magro, P. G. Mercadante, and S. F. Novaes, Phys. Rev. D 52 15-21 (1995).
- [15] İ. Sahin, J. Phys. G 36 075007 (2009).
- [16] T. Pierzchala and K. Piotrkowski, Nucl. Phys. Proc. Suppl. 179-180 257 (2008).
- [17] E. Chapon, C. Royon and O. Kepka, Phys. Rev. D 81 074003 (2010).
- [18] A. Senol, arXiv:1311.1370.
- [19] P. J. Bell, Eur. Phys. J. C 64 25-33 (2009).
- [20] O. J. P. Eboli, M. C. Gonzalez-Garcia, and S. M. Lietti, S. F. Novaes Phys. Rev. D 63 075008 (2001).
- [21] D. Yang, Y. Mao, Q. Li, S. Liu, Z. Xu, and K. Ye, arXiv:1211.1641.
- [22] O. J. P. Eboli, M. C. Gonzalez-Garcia, and S. M. Lietti, Phys. Rev. D 69 095005 (2004).
- [23] D. Dannheim *et al.*, CLIC e+e- Linear Collider Studies, arXiv:1305.5766v1.
- [24] D. Dannheim *et al.*, CLIC e⁺e⁻ Linear Collider Studies, arXiv:1208.1402.
- [25] I. F. Ginzburg, G. L. Kotkin, V. G. Serbo and V. I. Telnov, Nucl. Instr. and Meth. 205 47 (1983).

- [26] I. F. Ginzburg, G. L. Kotkin, S. L. Panfil, V. G. Serbo and V. I. Telnov, Nucl. Instr. and Meth. 219 5 (1984).
- [27] V. I. Telnov, Nucl. Instr. and Meth. A 294 72 (1990).
- [28] V.M. Budnev, I.F. Ginzburg, G.V. Meledin and V.G. Serbo, Phys. Rept. 15 181 (1974).
- [29] G. Baur *et al.*, Phys. Rep. 364 359 (2002).
- [30] E. Yehudai, Phys. Rev. D 41 33 (1990).
- [31] C. Carimalo, P. Kessler and J. Parisi, Phys. Rev. D 20 1057 (1979).
- [32] J.E. Cieza Montalvo, N. V. Cortez, M. D. Tonasse, Phys.Rev. D 77 095015 (2008).
- [33] R. Nisius, Phys. Rept. 332 165-317 (2000).
- [34] J. Abdallah *et al.*, DELPHI Collaboration, Eur. Phys. J. C 35 159 (2004).
- [35] A. Abulencia *et al.*, CDF Collaboration, Phys. Rev. Lett. 98 112001 (2007).
- [36] T. Aaltonen *et al.*, CDF Collaboration, Phys. Rev. Lett. 102 222002 (2009).
- [37] T. Aaltonen *et al.*, CDF Collaboration, Phys. Rev. Lett. 102 242001 (2009).
- [38] S. Chatrchyan *et al.*, CMS Collaboration, JHEP 1201 052 (2012).
- [39] S. Chatrchyan *et al.*, CMS Collaboration, JHEP 1211 080 (2012).
- [40] CMS Collaboration, JHEP 07 116 (2013).
- [41] S. Atag and A. Billur, JHEP 11 060 (2010).
- [42] K. Piotrkowski, Phys. Rev. D 63 071502 (2001).
- [43] H. Murayama and M. E. Peskin, Ann. Rev. Nucl. Part. Sci. 46 533-608 (1996).
- [44] S. Atag, S. C. İnan and İ. Şahin, Phys. Rev. D 80 075009 (2009).
- [45] İ. Şahin and S. C. İnan, JHEP 09 069 (2009).
- [46] S. C. İnan, Phys. Rev. D 81 115002 (2010).
- [47] İ. Şahin and M. Köksal, JHEP 11 100 (2011).
- [48] M. Köksal and S. C. İnan, arXiv:1305.7096.
- [49] M. Köksal and S. C. İnan, AHEP Volume 2014, Article ID 315826, 8 pages (2014).
- [50] M. Köksal, arXiv:1402.2915.
- [51] A. A. Billur and M. Köksal, Phys. Rev. D 89 037301 (2014).
- [52] A. A. Billur and M. Köksal, arXiv:1311.5326.
- [53] A. Senol, Phys. Rev. D 85 113015 (2012).
- [54] İ. Şahin *et al.*, Phys.Rev. D 88 095016 (2013).
- [55] S. C. İnan and A. Billur, Phys. Rev. D 84 095002 (2011).

- [56] R. S. Gupta, Phys. Rev. D 85014006 (2012).
- [57] İ. Şahin, Phys. Rev. D 85 033002 (2012).
- [58] L. N. Epele *et al.*, Eur. Phys. J. Plus 127 60 (2012).
- [59] İ. Şahin and B. Şahin, Phys. Rev. D 86 115001 (2012).
- [60] A. A. Billur, Europhys. Lett. 101 21001 (2013).
- [61] A. Pukhov *et al.*, Report No. INP MSU 98-41/542; arXiv:hep-ph/9908288; arXiv:hep-ph/0412191.

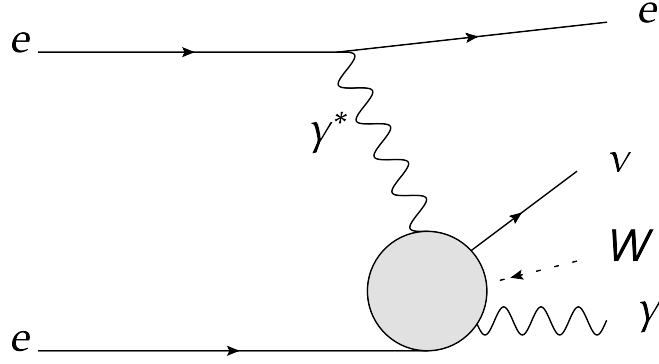


FIG. 1: Representative diagram for the reaction $e^+e^- \rightarrow e^+\gamma^*e^- \rightarrow e^+W^-\gamma\nu_e$.

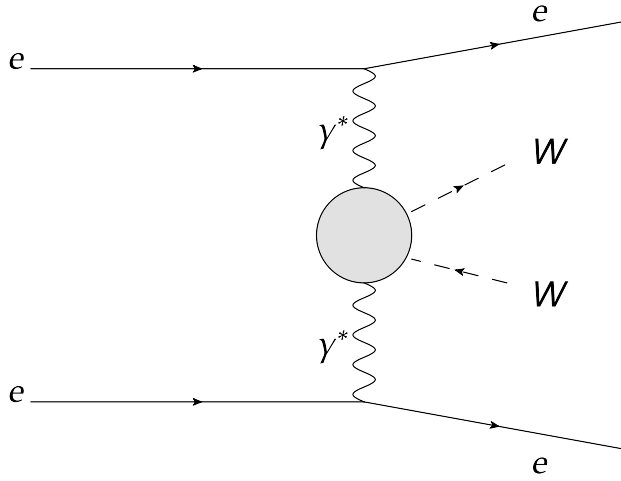


FIG. 2: Representative diagram for the reaction $e^+e^- \rightarrow e^+\gamma^*\gamma^*e^- \rightarrow e^+W^+W^-e^-$.

TABLE I: The fundamental parameters of the three energy options of the CLIC. Here \sqrt{s} is the center-of-mass energy, N is the number of particles in bunch, L is the total luminosity, $\sigma_{x,y,z}$ are the average sizes of the bunches [24].

Parameter	Unit	Stage 1	Stage 2	Stage 3
\sqrt{s}	TeV	0.5	1.5	3
N	10^9	3.7	3.7	3.7
L	fb^{-1}	230	320	590
σ_x	nm	100	60	40
σ_y	nm	2.6	1.5	1
σ_z	μm	44	44	44

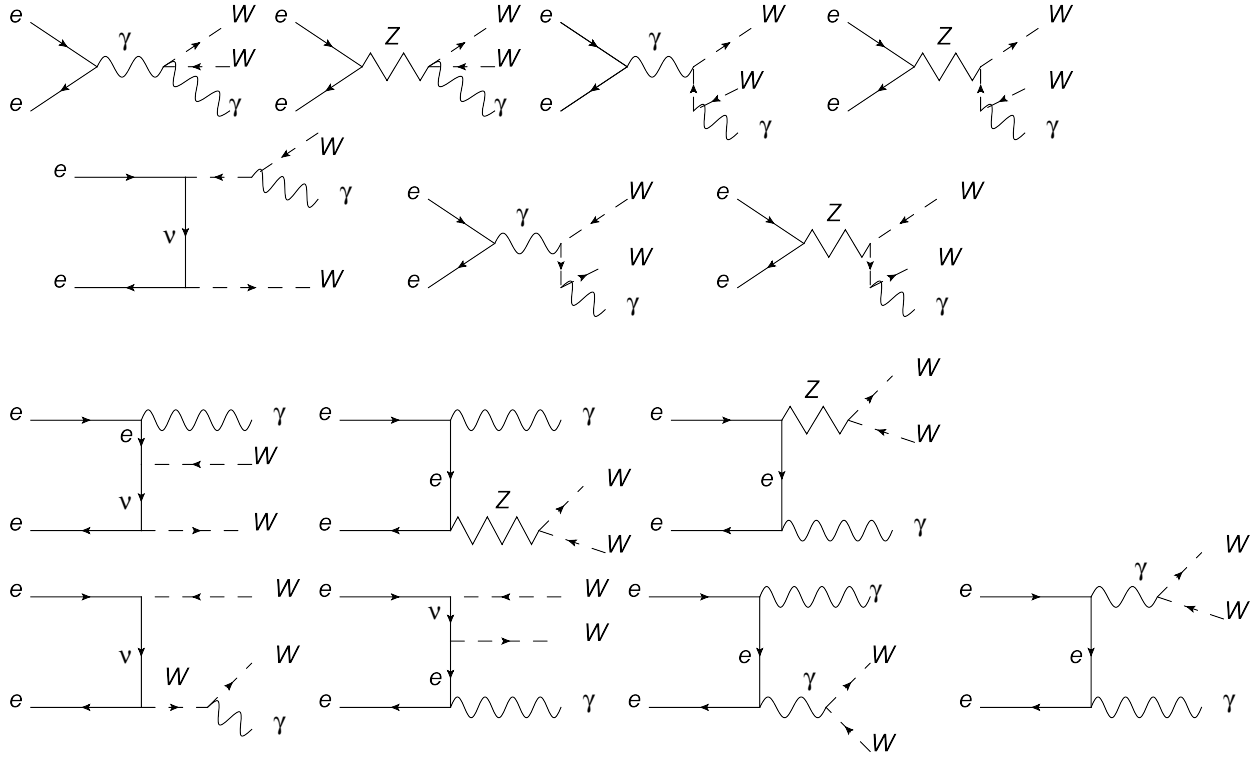


FIG. 3: Tree-level Feynman diagrams for the process $e^+e^- \rightarrow W^-W^+\gamma$.

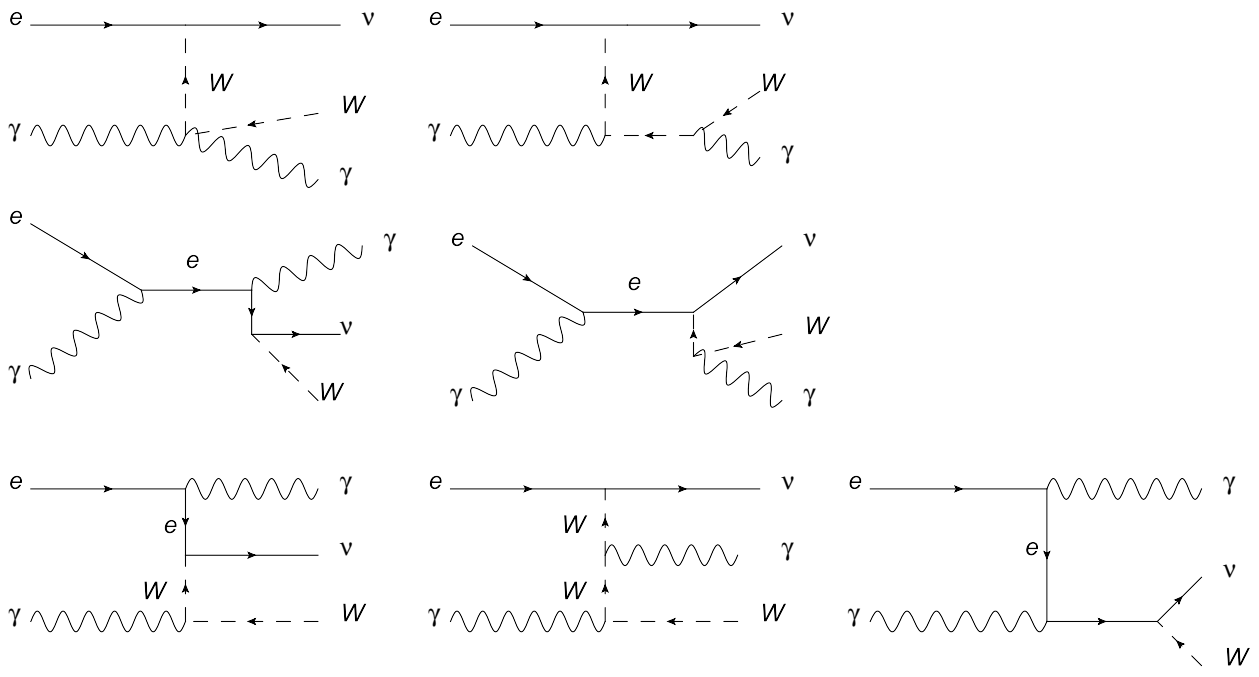


FIG. 4: Tree-level Feynman diagrams for the subprocess $e^-\gamma^* \rightarrow W^-\gamma\nu_e$.

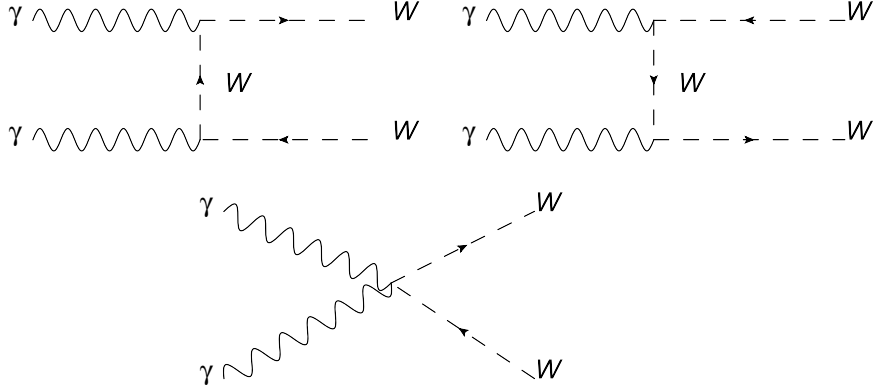


FIG. 5: Tree-level Feynman diagrams for the subprocess $\gamma^* \gamma^* \rightarrow W^- W^+$.

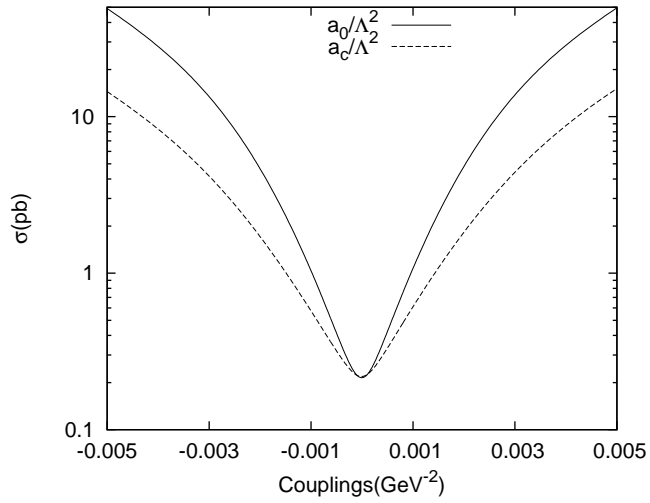


FIG. 6: The total cross sections as function of anomalous $\frac{a_0}{\Lambda^2}$ and $\frac{a_c}{\Lambda^2}$ couplings for the $e^+e^- \rightarrow W^-W^+\gamma$ at the CLIC with $\sqrt{s} = 0.5 \text{ TeV}$.

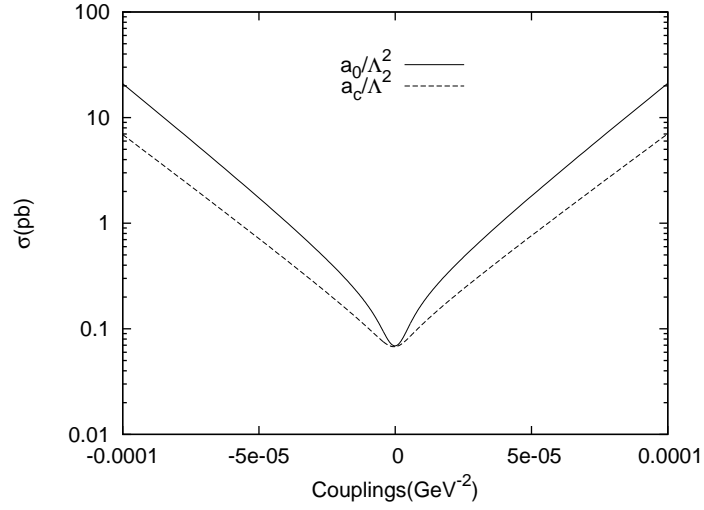


FIG. 7: The same as Fig. 6 but for $\sqrt{s} = 1.5$ TeV.

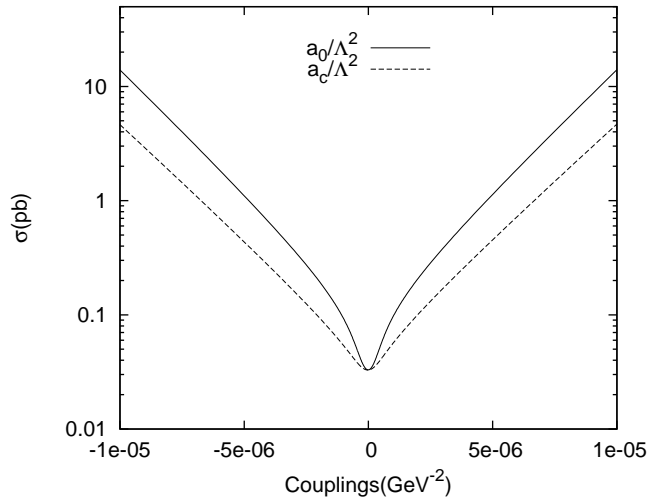


FIG. 8: The same as Fig. 6 but for $\sqrt{s} = 3$ TeV.

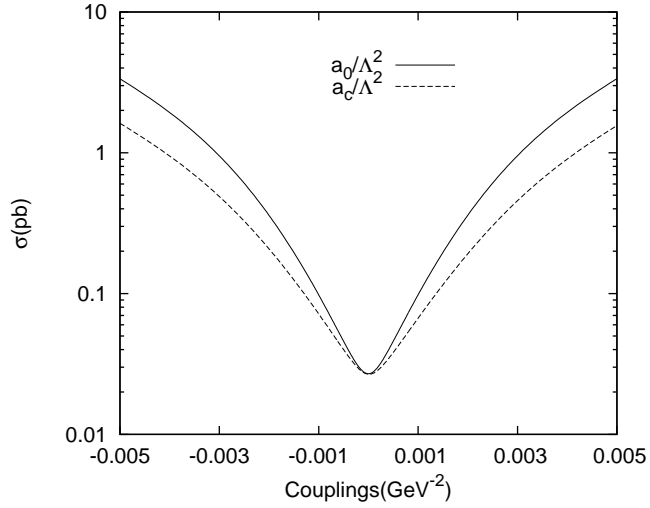


FIG. 9: The total cross sections as function of anomalous $\frac{a_0}{\Lambda^2}$ and $\frac{a_c}{\Lambda^2}$ couplings for the $e^+e^- \rightarrow e^+\gamma^*e^- \rightarrow e^+W^-\gamma\nu_e$ at the CLIC with $\sqrt{s} = 0.5$ TeV.

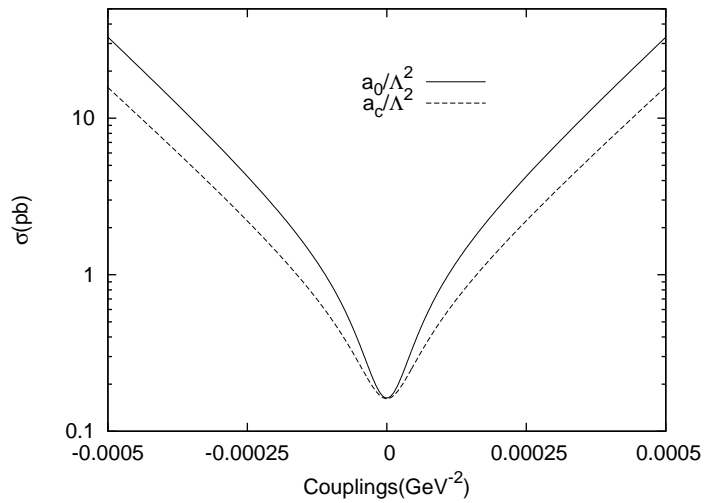


FIG. 10: The same as Fig. 9 but for $\sqrt{s} = 1.5$ TeV.

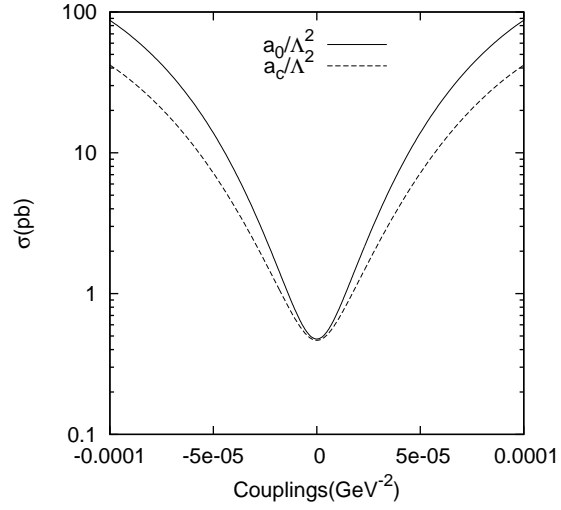


FIG. 11: The same as Fig. 9 but for $\sqrt{s} = 3$ TeV.

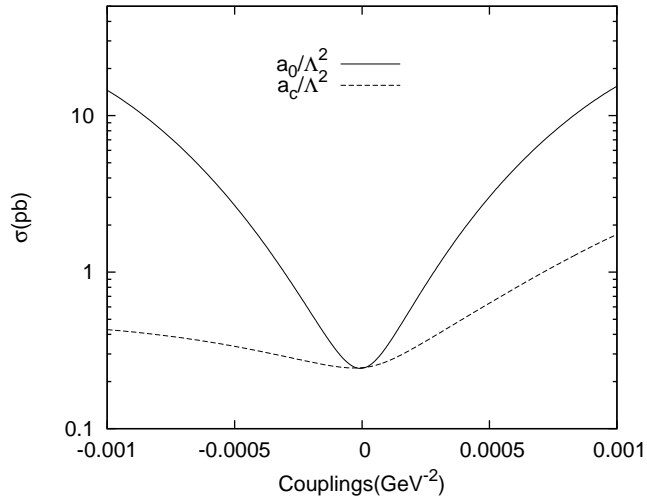


FIG. 12: The total cross sections as function of anomalous $\frac{a_0}{\Lambda^2}$ and $\frac{a_c}{\Lambda^2}$ couplings for the $e^+e^- \rightarrow e^+\gamma^*\gamma^*e^- \rightarrow e^+W^-W^+e^-$ at the CLIC with $\sqrt{s} = 0.5$ TeV.

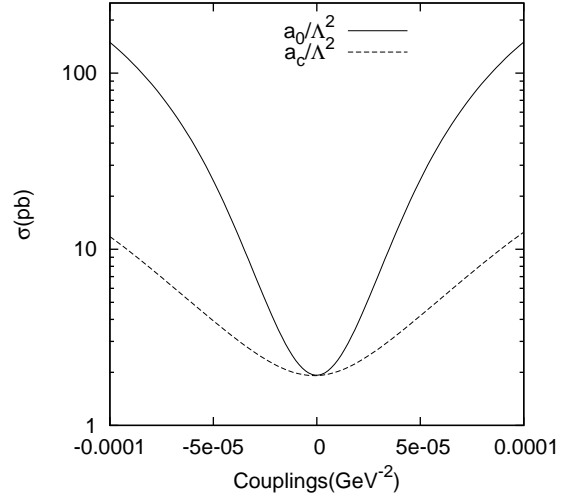


FIG. 13: The same as Fig. 12 but for $\sqrt{s} = 1.5$ TeV.

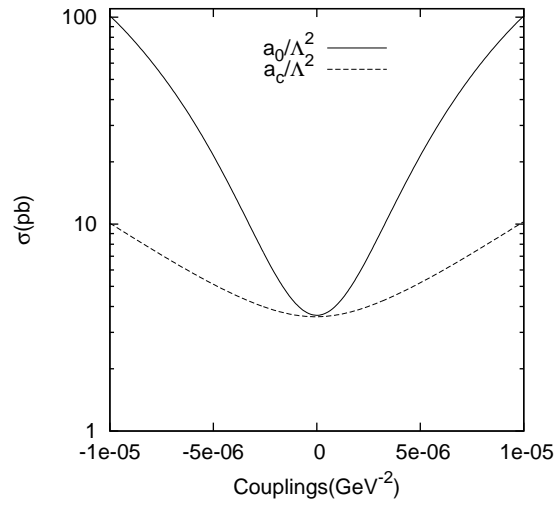


FIG. 14: The same as Fig. 12 but for $\sqrt{s} = 3$ TeV.

TABLE II: 95% C.L. sensitivity bounds of the $\frac{a_0}{\Lambda^2}$ and $\frac{a_c}{\Lambda^2}$ couplings through the processes $e^+e^- \rightarrow W^-W^+\gamma$ at the CLIC with $\sqrt{s} = 0.5, 1.5$ and 3 TeV.

\sqrt{s} (TeV)	$L_{int}(\text{fb}^{-1})$	$\frac{a_0}{\Lambda^2}(\text{GeV}^{-2})$	$\frac{a_c}{\Lambda^2}(\text{GeV}^{-2})$
0.5	10	$[-1.20 \times 10^{-4}, 0.93 \times 10^{-4}]$	$[-2.53 \times 10^{-4}, 1.41 \times 10^{-4}]$
0.5	50	$[-8.65 \times 10^{-5}, 5.44 \times 10^{-5}]$	$[-1.95 \times 10^{-4}, 8.13 \times 10^{-5}]$
0.5	100	$[-7.63 \times 10^{-5}, 4.41 \times 10^{-5}]$	$[-1.76 \times 10^{-4}, 6.50 \times 10^{-5}]$
0.5	230	$[-6.56 \times 10^{-5}, 3.37 \times 10^{-5}]$	$[-1.60 \times 10^{-4}, 4.93 \times 10^{-5}]$
1.5	10	$[-2.66 \times 10^{-6}, 2.25 \times 10^{-6}]$	$[-4.69 \times 10^{-6}, 3.83 \times 10^{-6}]$
1.5	100	$[-1.53 \times 10^{-6}, 1.16 \times 10^{-6}]$	$[-2.82 \times 10^{-6}, 1.98 \times 10^{-6}]$
1.5	200	$[-1.37 \times 10^{-6}, 0.95 \times 10^{-6}]$	$[-2.47 \times 10^{-6}, 1.61 \times 10^{-6}]$
1.5	320	$[-1.23 \times 10^{-6}, 0.83 \times 10^{-6}]$	$[-2.25 \times 10^{-6}, 1.38 \times 10^{-6}]$
3	10	$[-2.61 \times 10^{-7}, 2.33 \times 10^{-7}]$	$[-4.53 \times 10^{-7}, 3.96 \times 10^{-7}]$
3	100	$[-1.50 \times 10^{-7}, 1.34 \times 10^{-7}]$	$[-2.62 \times 10^{-7}, 2.22 \times 10^{-7}]$
3	300	$[-1.19 \times 10^{-7}, 9.39 \times 10^{-8}]$	$[-2.11 \times 10^{-7}, 1.58 \times 10^{-7}]$
3	590	$[-9.96 \times 10^{-8}, 7.27 \times 10^{-8}]$	$[-1.76 \times 10^{-7}, 1.31 \times 10^{-7}]$

TABLE III: 95% C.L. sensitivity bounds of the $\frac{a_0}{\Lambda^2}$ and $\frac{a_e}{\Lambda^2}$ couplings through the processes $e^+e^- \rightarrow e^+\gamma^*e^- \rightarrow e^+W^-\gamma\nu_e$ at the CLIC with $\sqrt{s} = 0.5, 1.5$ and 3 TeV.

\sqrt{s} (TeV)	$L_{int}(\text{fb}^{-1})$	$\frac{a_0}{\Lambda^2}(\text{GeV}^{-2})$	$\frac{a_e}{\Lambda^2}(\text{GeV}^{-2})$
0.5	10	$[-1.62 \times 10^{-4}, 1.58 \times 10^{-4}]$	$[-1.91 \times 10^{-4}, 2.86 \times 10^{-4}]$
0.5	50	$[-1.09 \times 10^{-4}, 1.04 \times 10^{-4}]$	$[-1.16 \times 10^{-4}, 2.11 \times 10^{-4}]$
0.5	100	$[-0.89 \times 10^{-4}, 0.86 \times 10^{-4}]$	$[-0.93 \times 10^{-4}, 1.84 \times 10^{-4}]$
0.5	230	$[-0.73 \times 10^{-4}, 0.71 \times 10^{-4}]$	$[-0.68 \times 10^{-4}, 1.61 \times 10^{-4}]$
1.5	10	$[-8.08 \times 10^{-6}, 8.02 \times 10^{-6}]$	$[-1.09 \times 10^{-5}, 1.27 \times 10^{-5}]$
1.5	50	$[-4.52 \times 10^{-6}, 4.48 \times 10^{-6}]$	$[-5.41 \times 10^{-6}, 7.45 \times 10^{-6}]$
1.5	100	$[-3.75 \times 10^{-6}, 3.71 \times 10^{-6}]$	$[-4.57 \times 10^{-6}, 6.63 \times 10^{-6}]$
1.5	230	$[-3.29 \times 10^{-6}, 3.24 \times 10^{-6}]$	$[-4.06 \times 10^{-6}, 6.12 \times 10^{-6}]$
3	10	$[-1.15 \times 10^{-6}, 1.12 \times 10^{-6}]$	$[-1.59 \times 10^{-6}, 1.71 \times 10^{-6}]$
3	100	$[-6.38 \times 10^{-7}, 6.32 \times 10^{-7}]$	$[-8.34 \times 10^{-7}, 9.76 \times 10^{-7}]$
3	300	$[-4.97 \times 10^{-7}, 4.93 \times 10^{-7}]$	$[-6.14 \times 10^{-7}, 7.59 \times 10^{-7}]$
3	590	$[-4.05 \times 10^{-7}, 4.02 \times 10^{-7}]$	$[-4.81 \times 10^{-7}, 6.82 \times 10^{-7}]$

TABLE IV: 95% C.L. sensitivity bounds of the $\frac{a_0}{\Lambda^2}$ and $\frac{a_c}{\Lambda^2}$ couplings for $e^+e^- \rightarrow e^+\gamma^*\gamma^*e^- \rightarrow e^+W^-W^+e^-$ at the CLIC with $\sqrt{s} = 0.5, 1.5$ and 3 TeV.

\sqrt{s} (TeV)	$L_{int}(\text{fb}^{-1})$	$\frac{a_0}{\Lambda^2}(\text{GeV}^{-2})$	$\frac{a_c}{\Lambda^2}(\text{GeV}^{-2})$
0.5	10	$[-5.78 \times 10^{-5}, 2.78 \times 10^{-5}]$	$[-3.21 \times 10^{-4}, 5.91 \times 10^{-5}]$
0.5	50	$[-4.58 \times 10^{-5}, 1.54 \times 10^{-5}]$	$[-2.93 \times 10^{-4}, 2.95 \times 10^{-5}]$
0.5	100	$[-4.25 \times 10^{-5}, 1.18 \times 10^{-5}]$	$[-2.86 \times 10^{-4}, 2.15 \times 10^{-5}]$
0.5	230	$[-3.89 \times 10^{-5}, 0.85 \times 10^{-5}]$	$[-2.79 \times 10^{-4}, 1.48 \times 10^{-5}]$
1.5	10	$[-2.21 \times 10^{-6}, 1.90 \times 10^{-6}]$	$[-9.38 \times 10^{-6}, 6.22 \times 10^{-6}]$
1.5	100	$[-1.31 \times 10^{-6}, 1.03 \times 10^{-6}]$	$[-6.07 \times 10^{-6}, 2.96 \times 10^{-6}]$
1.5	200	$[-1.14 \times 10^{-6}, 0.83 \times 10^{-6}]$	$[-5.57 \times 10^{-6}, 2.42 \times 10^{-6}]$
1.5	320	$[-1.04 \times 10^{-6}, 0.75 \times 10^{-6}]$	$[-5.18 \times 10^{-6}, 1.95 \times 10^{-6}]$
3	10	$[-3.11 \times 10^{-7}, 2.98 \times 10^{-7}]$	$[-1.22 \times 10^{-6}, 1.08 \times 10^{-6}]$
3	100	$[-1.76 \times 10^{-7}, 1.68 \times 10^{-7}]$	$[-7.31 \times 10^{-7}, 5.85 \times 10^{-7}]$
3	300	$[-1.40 \times 10^{-7}, 1.31 \times 10^{-7}]$	$[-5.90 \times 10^{-7}, 4.35 \times 10^{-7}]$
3	590	$[-1.08 \times 10^{-7}, 1.02 \times 10^{-7}]$	$[-4.99 \times 10^{-7}, 3.41 \times 10^{-7}]$